Synthesis, Structure, and Dynamic Behavior of Rhenium Sulfide and Sulfoxide Complexes of the Formula [(η⁵-C₅H₅)Re(NO)(L)(XRR')]⁺X'⁻ (X = S, SO)

N. Quirós Méndez, Atta M. Arif, and J. A. Gladysz*

Department of Chemistry, University of Utah, Salt Lake City, Utah 84112

Reactions of $(\eta^5\text{-}C_5H_5)Re(NO)(PPh_3)(OTf)$ and sulfides MeSR (R = Me (**a**), Et (**b**), *i*-Pr (**c**), *t*-Bu (**d**)) give sulfide complexes $[(\eta^5\text{-}C_5H_5)Re(NO)(PPh_3)(S(R)Me)]^+TfO^-$ (**2a**–**d**⁺TfO⁻; 91–51%). Reactions of $[(\eta^5\text{-}C_5H_5)Re(NO)(PPh_3)(ClCH_2Cl)]^+BF_4^-$ with SMe₂ and O=SMe₂ give **2a**⁺BF₄⁻ (64%) and DMSO complex $[(\eta^5\text{-}C_5H_5)Re(NO)(PPh_3)(S(=O)Me_2)]^+BF_4^-$ (**4a**⁺BF₄⁻; 86%). Reaction of **4a**⁺BF₄⁻ and excess SMe₂ gives **2a**⁺BF₄⁻ (83%). Reactions of $(\eta^5\text{-}C_5H_5)Re(NO)(CO)(OTf)$ with SMe₂ and S(*t*-Bu)₂ give carbonyl-substituted sulfide complexes $[(\eta^5\text{-}C_5H_5)Re(NO)(CO)(SR_2)]^+TfO^-$ (**6a**,**e**⁺TfO⁻; 99–81%). Sulfide complexes **2a**⁺TfO⁻ and **6a**,**e**⁺TfO⁻ exhibit dynamic NMR behavior ($\Delta G^\ddagger(T_c)$ = 9.5–12.9 kcal/mol) arising from inversion of configuration at sulfur. Crystal structures of **2a**⁺TfO⁻·CH₂Cl₂ (monoclinic, $P2_1/n$, *a* = 8.254 (2) Å, *b* = 27.429 (8) Å, *c* = 13.782 (7) Å, β = 96.67 (3)°, Z = 4), **4a**⁺BF₄⁻ (triclinic, $P\bar{1}$, *a* = 10.472 (1) Å, *b* = 14.162 (2) Å, *c* = 9.441 (1) Å, α = 101.036 (3)°, β = 90.891 (3)°, γ = 87.781 (3), Z = 4), and **6a**⁺TfO⁻ (monoclinic, $P2_1/n$, *a* = 8.346 (2) Å, *b* = 25.387 (10) Å, *c* = 7.287 (2) Å, β = 96.95 (3)°, Z = 4) are reported. The sulfoxide oxygen in **4a**⁺BF₄⁻ is syn to the PPh₃ ligand (torsion angle P–Re–S–O = 17°).

Transition-metal complexes of dialkyl sulfides are ubiquitous.[1] Diverse aspects of their physical and chemical properties have attracted the attention of researchers.[1–6] These include rich conformational and configurational dynamics,[2] reactivity models for catalytic hydrodesulfurization,[3] structural and electronic analogues of sulfur-ligated metalloenzymes,[4] binding units in macrocyclic ligand complexes,[5] and vehicles for the asymmetric oxidation of sulfides to sulfoxides.[6]

We have had an ongoing interest in the synthesis, structure, and reactivity of adducts of donor ligands and the chiral rhenium fragment $[(\eta^5\text{-}C_5H_5)Re(NO)(PPh_3)]^+$ (I).[7,8] In particular, many reactions have been found in which the rhenium chirality is efficiently transferred to a new ligand-based chiral center.[9] As a prelude to studies involving reactions *on* sulfur-containing ligands, we sought to define preparative routes to sulfide and sulfoxide com-

Scheme I. Synthesis of Phosphine-Substituted Sulfide Complexes 2⁺TfO⁻
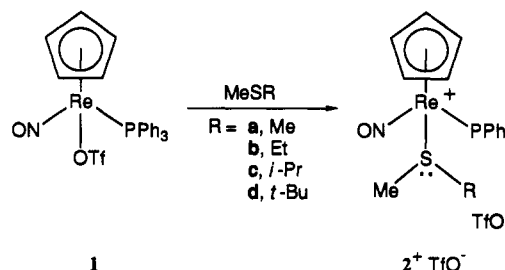
plexes and fundamental physical properties.

In this paper, we report (1) high-yield syntheses of chiral sulfide complexes $[(\eta^5\text{-}C_5H_5)Re(NO)(L)(SRR')]^+X^-$ (L = PPh₃, CO), (2) dynamic NMR studies that establish some of the lowest known sulfur inversion barriers, (3) crystal structures of two dimethyl sulfide complexes, and (4) preliminary studies, including a crystal structure, of analogous sulfoxide complexes.
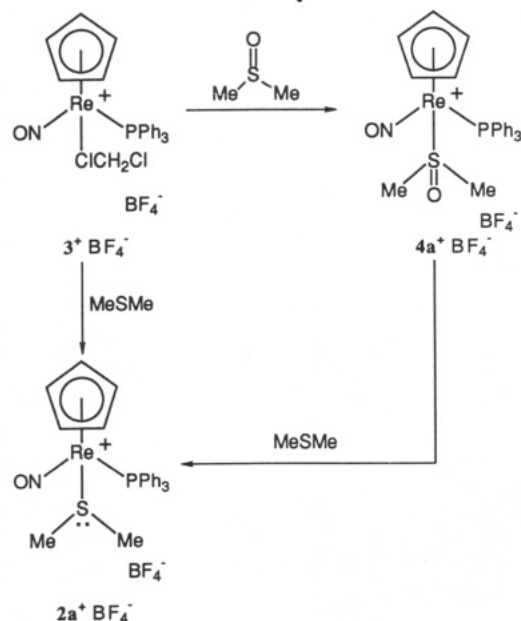
Results

1. Synthesis of Sulfide Complexes. Triflate complex $(\eta^5\text{-}C_5H_5)Re(NO)(PPh_3)(OTf)$ (**1**)[10] and sulfides MeSR (R = Me (**a**), Et (**b**), *i*-Pr (**c**), *t*-Bu (**d**); ca. 5 equiv) were reacted in CH₂Cl₂ (Scheme I). Workup gave sulfide complexes $[(\eta^5\text{-}C_5H_5)Re(NO)(PPh_3)(S(R)Me)]^+TfO^-$ (**2a**–**d**⁺TfO⁻). Methyl *tert*-butyl sulfide complex **2d**⁺TfO⁻ was isolated in somewhat lower yield (51%) than **2a**–**c**⁺TfO⁻ (81–91%). No reaction occurred when **1** and bis(*tert*-butyl) sulfide were combined under similar conditions, as assayed by IR spectroscopy.

Complexes **2a**–**d**⁺TfO⁻, and all other new compounds isolated below, were characterized by microanalysis (Experimental Section) and IR and NMR (¹H, ¹³C{¹H}, ³¹P{¹H}) spectroscopy (Table I). General features were similar to those previously reported for other adducts of I and neutral heteroatomic Lewis bases, such as alcohol and ether complexes $[(\eta^5\text{-}C_5H_5)Re(NO)(PPh_3)(ORR')]^+X^-$.[8b,d] Importantly, the diastereotopic methyl groups in **2a**⁺TfO⁻ gave

(1) Murray, S. G.; Hartley, F. R. *Chem. Rev.* 1981, *81*, 365.

(2) (a) Abel, E. W.; Bhargava, S. K.; Orrell, K. G. *Prog. Inorg. Chem.* 1984, *32*, 1. (b) Abel, E. W.; Moss, I.; Orrell, K. G.; Sik, V. *J. Organomet. Chem.* 1987, *326*, 187. (c) Abel, E. W. *Chem. Britain* 1990, 148.

(3) (a) Angelici, R. J. *Acc. Chem. Res.* 1988, *21*, 388. (b) Rakowski, Dubois, M. *Chem. Rev.* 1989, *89*, 1.

(4) (a) Cooper, S. R. *Acc. Chem. Res.* 1988, *21*, 141. (b) Bernardo, M. M.; Robandt, P. V.; Schroeder, R. R.; Rorabacher, D. B. *J. Am. Chem. Soc.* 1989, *111*, 1224.

(5) Some lead references: (a) Blake, A. J.; Schröder, M. *Adv. Inorg. Chem.* 1990, *35*, 1. (b) Desper, J. M.; Gellman, S. H. *J. Am. Chem. Soc.* 1990, *112*, 6732. (c) Yoshida, T.; Adachi, T.; Ueda, T.; Tanaka, T.; Goto, F. *J. Chem. Soc., Chem. Commun.* 1990, 342.

(6) (a) Pitchen, P.; Duñach, E.; Deshmukh, M. N.; Kagan, H. B. *J. Am. Chem. Soc.* 1984, *106*, 8188. (b) Samuel, O.; Ronan, B.; Kagan, H. B. *J. Organomet. Chem.* 1989, *379*, 43.

(7) (a) Fernández, J. M.; Gladysz, J. A. *Organometallics* 1989, *8*, 207. (b) Kowalczyk, J. J.; Agbossou, S. K.; Gladysz, J. A. *J. Organomet. Chem.* 1990, *397*, 333.

(8) Recent lead references: (a) Winter, C. H.; Veal, W. R.; Garner, C. M.; Arif, A. M.; Gladysz, J. A.; *J. Am. Chem. Soc.* 1989, *111*, 4766. (b) Agbossou, S. K.; Fernández, J. M.; Gladysz, J. A. *Inorg. Chem.* 1990, *29*, 476. (c) Bodner, G. S.; Peng, T.-S.; Arif, A. M.; Gladysz, J. A. *Organometallics* 1990, *9*, 1191. (d) Agbossou, S. K.; Smith, W. W.; Gladysz, J. A. *Chem. Ber.* 1990, *123*, 1293. (e) Dewey, M. A.; Bakke, J. M.; Gladysz, J. A. *Organometallics* 1990, *9*, 1349. (f) Kowalczyk, J. J.; Arif, A. M.; Gladysz, J. A. *Organometallics* 1991, *10*, 1079.

(9) (a) Garner, C. M.; Quirós Méndez, N.; Kowalczyk, J. J.; Fernández, J. M.; Emerson, K.; Larsen, R. D.; Gladysz, J. A. *J. Am. Chem. Soc.* 1990, *112*, 5146. (b) Peng, T.-S.; Gladysz, J. A. *Tetrahedron Lett.* 1990, *31*, 4417. (c) Dalton, D. M.; Fernández, J. M.; Emerson, K.; Larsen, R. D.; Arif, A. M.; Gladysz, J. A. *J. Am. Chem. Soc.* 1990, *112*, 9198.

(10) (a) Merrifield, J. H.; Fernández, J. M.; Buhro, W. E.; Gladysz, J. A. *Inorg. Chem.* 1984, *23*, 4022. (b) TfO⁻ = CF₃SO₃⁻.

Scheme II. Synthesis and Reaction of Sulfoxide Complex
4a⁺BF₄⁻

only one ¹H and ¹³C NMR resonance at room temperature. Also, complexes **2b–d⁺TfO⁻** contain two stereocenters (rhenium and sulfur) and, hence, can in principle exist as mixtures of diastereomers. However, only one set of NMR resonances was observed. Additional NMR experiments are described below.

An alternative route to sulfide complexes **2⁺X⁻** was briefly probed. The substitution-labile dichloromethane complex [(η^5-C₅H₅)Re(NO)(PPh₃)(ClCH₂Cl)]⁺BF₄⁻ (**3⁺-BF₄⁻**) was generated at −80 °C, as previously described (Scheme II).[7a] Then dimethyl sulfide was added (3 equiv). Workup gave dimethyl sulfide complex **2a⁺BF₄⁻** in 64% yield. The ¹H NMR spectrum of **2a⁺BF₄⁻** was identical with that of **2a⁺TfO⁻**. When the preceding reaction was monitored by ³¹P NMR spectroscopy, **2a⁺BF₄⁻** was observed to form in quantitative yield over the temperature range −40 °C to 0 °C.

2. Crystal Structure of 2a⁺TfO⁻·CH₂Cl₂. In order to help interpret the dynamic properties suggested by the preceding NMR data, a crystal structure of a sulfide complex was sought. Yellow prisms of a solvate, **2a⁺-TfO⁻·CH₂Cl₂**, were obtained from CH₂Cl₂/ether. X-ray data were collected under the conditions summarized in Table II. Refinement (Experimental Section) gave the structures shown in Figure 1.

The sulfide ligand sulfur atom was pyramidal, and a lone-pair (LP) position was calculated. The atomic coordinates of **2a⁺TfO⁻·CH₂Cl₂** and key bond lengths, bond angles, and torsion angles are summarized in Tables III and IV. A complete listing of bond lengths and angles is given elsewhere.[11]

3. Synthesis and Properties of Sulfoxide Complexes. Pursuant to projected studies of the oxidation of sulfide complexes **2⁺X⁻**, data on the physical and chemical properties of analogous sulfoxide complexes were sought. Thus, the dichloromethane complex **3⁺BF₄⁻** was treated with dimethyl sulfoxide (DMSO; Scheme II). Workup gave the DMSO complex [(η^5-C₅H₅)Re(NO)(PPh₃)(S(=O)-Me₂)]⁺BF₄⁻ (**4a⁺BF₄⁻**) in 86% yield.

The DMSO complex **4a⁺BF₄⁻** exhibited separate ¹H and ¹³C NMR resonances for the diastereotopic methyl groups.

---

(11) Quirós Méndez, N. Ph.D. Thesis, University of Utah, 1991.
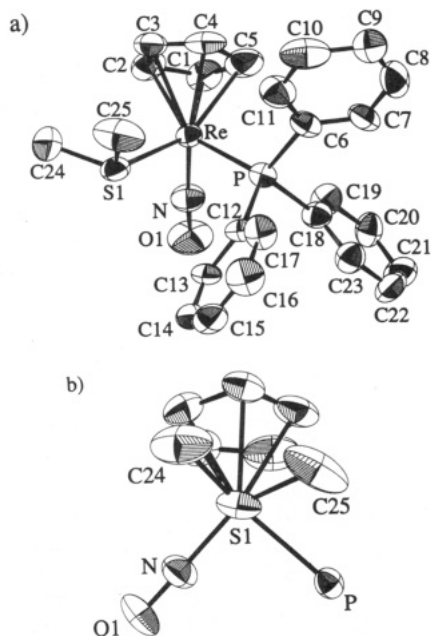
Figure 1. Structure of the cation of dimethyl sulfide complex [(η^5-C₅H₅)Re(NO)(PPh₃)(SMe₂)]⁺TfO⁻·CH₂Cl₂ (**2a⁺TfO⁻·CH₂Cl₂**): (a) numbering diagram; (b) Newman-type projection with phenyl rings omitted.
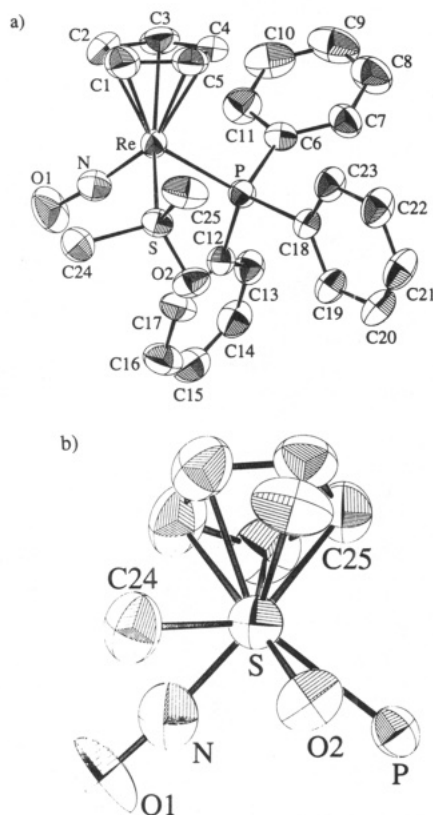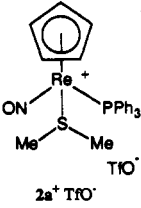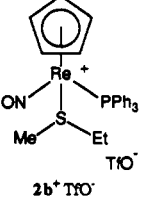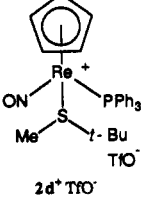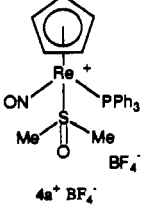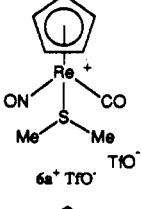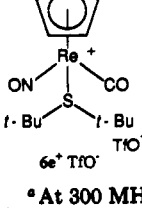
Figure 2. Structure of the cation of dimethyl sulfoxide complex [(η^5-C₅H₅)Re(NO)(PPh₃)(S(=O)Me₂)]⁺BF₄⁻ (**4a⁺BF₄⁻**): (a) numbering diagram; (b) Newman-type projection with phenyl rings omitted.

It also gave an IR ν_{SO} absorption (1123 cm⁻¹) in a range considered diagnostic of sulfur, as opposed to oxygen, coordination.[12] This assignment was verified by a crystal

---

(12) (a) Reynolds, W. L. *Prog. Inorg. Chem.* **1970**, *12*, 1. (b) White, C.; Thopmson, S. J.; Maitlis, P. M. *J. Chem. Soc., Dalton Trans.* **1977**, 1654.

Table I. Spectroscopic Characterization of New Sulfide and Sulfoxide Complexes

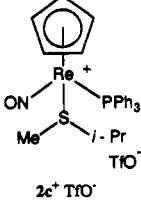| complex	IR (KBr), cm⁻¹	¹H NMR, δ[a]	¹³C{¹H} NMR, ppm[b]	³¹P{¹H} NMR, ppm[c]
2a⁺ TfO⁻	ν_{NO} 1716 vs	7.55–7.52 (m, 9 H of 3 C₆H₅), 7.30–7.24 (m, 6 H of 3 C₆H₅), 5.66 (s, C₅H₅), 2.55 (s, CH₃)	PPh₃ at 133.0 (d, J = 10.3, o), 132.4 (d, J = 55.9, i), 131.6 (s, p), 129.3 (d, J = 10.5, m); 92.8 (s, C₅H₅), 32.2 (d, J = 2.6, CH₃)	11.89 (s)
2b⁺ TfO⁻	ν_{NO} 1704 vs	7.54–7.52 (m, 9 H of 3 C₆H₅), 7.30–7.27 (m, 6 H of 3 C₆H₅), 5.65 (s, C₅H₅), 2.84 (q, J = 7.3, CH₂), 2.40 (s, SCH₃), 1.17 (t, J = 7.4, CH₂C*H₃*)	PPh₃ at 133.1 (d, J = 11.3, o), 132.3 (d, J = 55.9, i), 131.6 (d, J = 1.6, p), 129.2 (d, J = 10.3, m); 92.7 (s, C₅H₅), 43.1 (d, J = 1.6, CH₂), 27.7 (s, SCH₃), 13.6 (s, CH₂*C*H₃)	11.69 (s)
2c⁺ TfO⁻	ν_{NO} 1708 vs	7.54–7.50 (m, 9 H of 3 C₆H₅), 7.32–7.24 (m, 6 H of 3 C₆H₅), 5.65 (s, C₅H₅), 3.11 (sp, J = 6.6, SCH), 2.21 (s, SCH₃), 1.40 (d, J = 6.6, CHC*H₃*), 1.30 (d, J = 6.7, CHC′*H₃*)	PPh₃ at 133.1 (d, J = 11.4, o), 132.4 (d, J = 55.9, i), 131.6 (d, J = 2.6, p), 129.2 (d, J = 11.3, m); 92.8 (s, C₅H₅), 50.3 (d, J = 2.6, SCH), 24.0 (s, SCH₃), 21.5 (s, CH*C*H₃), 21.2 (s, CHC′*C*H₃)	11.12 (s)
2d⁺ TfO⁻	ν_{NO} 1700 vs	7.54–7.52 (m, 9 H of 3 C₆H₅), 7.34–7.23 (m, 6 H of 3 C₆H₅), 5.62 (s, C₅H₅), 2.08 (s, SCH₃), 1.38 (s, C(CH₃)₃)	PPh₃ at 133.1 (d, J = 10.2, o), 132.3 (d, i),[d] 131.5 (d, J = 2.3, p), 129.1 (d, J = 11.9, m); 92.4 (s, C₅H₅), 54.6 (d, J = 3.5, *C*(CH₃)₃), 28.3 (s, C(*C*H₃)₃), 22.4 (s, SCH₃)	11.02 (s)
4a⁺ BF₄⁻	ν_{NO} 1718 vs, ν_{SO} 1121 m[e]	7.57–7.42 (m, 3 C₆H₅), 5.67 (s, C₅H₅), 3.53 (s, CH₃), 3.31 (s, C′H₃)[f]	PPh₃ at 133.9 (d, J = 11.0, o), 132.8 (d, J = 57.6, i), 132.1 (d, J = 2.2, p), 129.5 (d, J = 11.3, m); 94.4 (s, C₅H₅), 56.2 (s, CH₃), 52.8 (s, C′H₃)[f]	9.31 (s)[f]
6a⁺ TfO⁻	ν_{CO} 2014 vs, ν_{NO} 1738 vs	6.16 (s, C₅H₅), 3.05 (br s, CH₃)	193.1 (s, CO), 121.2 (q, J_{CF} = 321.0, CF₃), 94.7 (s, C₅H₅), 32.6 (br s, CH₃)	
6e⁺ TfO⁻	ν_{CO} 2002 vs, ν_{NO} 1746 vs	6.21 (s, C₅H₅), 1.64 (s, CH₃)	195.4 (s, CO), 120.7 (q, J_{CF} = 320.1, CF₃), 95.2 (s, C₅H₅), 61.6 (s, *C*CH₃), 32.6 (s, CH₃)	

[a] At 300 MHz in CDCl₃ at ambient probe temperature and referenced to internal Si(CH₃)₄ unless noted. All coupling constants are in Hz. [b] At 75 MHz in CDCl₃ at ambient probe temperature and referenced to CDCl₃ (77.0 ppm) unless noted. All couplings are in Hz and to ³¹P unless noted. Triflate carbon resonances are not observed in all cases. Assignments of phenyl carbon resonances are made as described in footnote c of Table I in: Buhro, W. E.; Georgiou, S.; Fernández, J. M.; Patton, A. T.; Strouse, C. E.; Gladysz, J. A. *Organometallics* **1986**, *5*, 956. [c] At 121 MHz in CDCl₃ at ambient probe temperature and referenced to external 85% H₃PO₄. [d] Part of *ipso* doublet obscured by PPh₃. [e] This band is a shoulder on a BF₄⁻ absorbance. The assignment was confirmed by a spectrum of 4a⁺TfO⁻ (1123 cm⁻¹). [f] Spectrum in CD₂Cl₂ (vs Si(C*H₃*)₄ at δ 0.00 or CD₂Cl₂ at 53.8 ppm) due to poor CDCl₃ solubility.

Table II. Summary of Crystallographic Data for Dimethyl Sulfide Complexes [(η^5-C$_5$H$_5$)Re(NO)(PPh$_3$)(SMe$_2$)]$^+$TfO$^-$•CH$_2$Cl$_2$ (2a$^+$TfO$^-$•CH$_2$Cl$_2$) and [(η^5-C$_5$H$_5$)Re(NO)(CO)(SMe$_2$)]$^+$TfO$^-$ (6a$^+$TfO$^-$) and DMSO Complex [(η^5-C$_5$H$_5$)Re(NO)(PPh$_3$)(S(=O)Me$_2$)]$^+$BF$_4^-$ (4a$^+$BF$_4^-$)

	2a$^+$TfO$^-$•CH$_2$Cl$_2$	4a$^+$BF$_4^-$	6a$^+$TfO$^-$
molecular formula	C$_{27}$H$_{28}$Cl$_2$F$_3$NO$_4$PS$_2$Re	C$_{25}$H$_{26}$NO$_2$BPSF$_4$Re	C$_9$H$_{11}$NO$_5$S$_2$F$_3$Re
fw	839.7	708.53	520.51
cryst system	monoclinic	triclinic	monoclinic
space group	$P2_1/n$	$P\bar{1}$	$P2_1/n$
cell dimens (16 °C)			
a, Å	8.254 (2)	10.472 (1)	8.346 (2)
b, Å	27.429 (8)	14.162 (2)	25.387 (10)
c, Å	13.782 (7)	9.441 (1)	7.287 (2)
α, deg		101.036 (3)	
β, deg	96.67 (3)	90.891 (3)	96.95 (3)
γ, deg		87.781 (3)	
V, Å^3	3099.3 (1)	1373.2 (1)	1532.6 (1)
Z	4	4	4
d_{calcd}, g/cm^3	1.80	1.71	2.26
d_{obs}, g/cm^3 (22 °C)	1.86 (CCl$_4$/CBr$_4$)	1.70 (CCl$_4$/CH$_2$I$_2$)	2.26 (CCl$_4$/CBr$_4$)
cryst dimens, mm	0.50 × 0.24 × 0.23	0.35 × 0.26 × 0.13	0.25 × 0.25 × 0.17
radiation (λ, Å)	Mo Kα (0.710 73)	Mo Kα (0.710 73)	Mo Kα (0.710 73)
data collcn method	θ-2θ	θ-2θ	θ-2θ
scan speed, deg/min	3–10, variable	3.0	2.5–8.0, variable
range/indices (h,k,l)	0,10; 0,30; −16,16	0,11; −15,15; −10,10	0,9; 0,27; −8,8
2θ scan range, deg	3 ≤ 2θ ≤ 51	2 ≤ 2θ ≤ 47	3 ≤ 2θ ≤ 48
no. of reflcns measd	6516	4153	2682
scan range	2θ(Kα_1) − 1.0 to 2θ(Kα_2) + 1.0	2θ(Kα_1) − 1.3 to 2θ(Kα_2) + 1.6	2θ(Kα_1) − 1.0 to 2θ(Kα_2) + 1.0
tot. bkgd/scan time	0.5	0.0	0.5
no. of reflcns between stds	97	98	98
tot. no. of unique data	5725	3977	2210
no. of obsd data, $I > 3\sigma(I)$	4406	3594	1659
min transm factor	0.8597	0.7881	0.5382
max transm factor	0.9987	0.9943	0.9943
no. of variables	370	326	181
abs coeff (μ), cm^{-1}	43.8	46.6	83.5
$R = \sum(||F_o| - |F_c||)/\sum|F_o|$	0.048	0.030	0.0434
$R_w = [\sum w(|F_o| - |F_c|)^2/\sum w|F_o|^2]^{1/2}$	0.066	0.037	0.0471
goodness of fit	1.60	1.80	3.22
weighting factor, w	unit weight	unit weight	unit weight
$\Delta\rho$(max), e Å^{-3}	1.09, <1.0 Å from Re	1.3, <0.9 Å from Re	1.37, <1.2 Å from Re

structure (Figure 2), which was executed similarly to that of **2a$^+$TfO$^-$**. Interestingly, the sulfoxide oxygen was syn to the PPh$_3$ ligand. Structural data are summarized in Tables III and IV.

We sought to probe the relative thermodynamic binding affinity of sulfides and sulfoxides for the rhenium fragment **I**. First, DMSO complex **4a$^+$BF$_4^-$** was suspended in chlorobenzene and treated with a large excess of dimethyl sulfide at 65 °C. Sulfide complex **2a$^+$BF$_4^-$** was subsequently isolated in 83% yield (Scheme II). Next, **4a$^+$BF$_4^-$** (0.029 mmol) was suspended in chlorobenzene-d_5 (0.60 mL) and treated with 3 equiv of dimethyl sulfide. The tube was sealed, kept at 65 °C, and periodically monitored by ^{31}P NMR spectroscopy. Over the course of 16 h, the concentration of **2a$^+$BF$_4^-$** increased while that of partially soluble **4a$^+$BF$_4^-$** remained constant (ratio: (87 ± 2):(13 ± 2)). After 7 days, no **4a$^+$BF$_4^-$** remained, but **2a$^+$BF$_4^-$** was accompanied by an approximately equal amount of a by-product (25.9 ppm). Nonetheless, the absence of **4a$^+$BF$_4^-$** in this dimethyl sulfide/DMSO ligand pool strongly suggests that dimethyl sulfide has a higher thermodynamic binding affinity for **I** than DMSO.[13]

Finally, dichloromethane complex **3$^+$BF$_4^-$** was treated with a chiral sulfoxide, benzyl methyl sulfoxide (3 equiv). Analysis of the resulting crude adduct [(η^5-C$_5$H$_5$)Re-(NO)(PPh$_3$)(S(=O)(CH$_2$Ph)Me)]$^+$BF$_4^-$ (**4e$^+$BF$_4^-$**) by ^{1}H

Scheme III. Synthesis of Carbonyl-Substituted Sulfide Complexes 6$^+$TfO$^-$
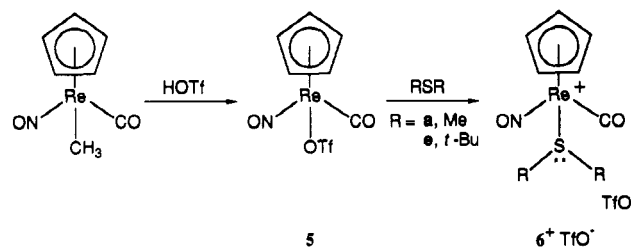
NMR spectroscopy indicated a (58 ± 3):(42 ± 3) mixture of Re/S configurational diastereomers (δ, CD$_2$Cl$_2$, major/minor: 5.74/5.64, C$_5$H$_5$; 3.17/3.07, Me). Thus, only a modest degree of chiral recognition occurred. The characterization of this inhomogeneous sample was not pursued further.

4. Carbonyl-Substituted Sulfide Complexes. The carbonyl-substituted rhenium fragment [(η^5-C$_5$H$_5$)Re-(NO)(CO)]$^+$ (**II**) is a somewhat weaker π base than **I**[14,15] and possesses a "pseudo" mirror plane that reflects the carbonyl ligand into the "isosteric" nitrosyl ligand. We sought to briefly explore the properties of sulfide complexes of **II**. Thus, the methyl complex (η^5-C$_5$H$_5$)Re-(NO)(CO)(CH$_3$)[16] and TfOH were reacted to give triflate

(13) Similar equilibrations were attempted under homogeneous conditions in CD$_2$Cl$_2$. However, the 25.9 ppm byproduct formed faster than substitution product **2a$^+$BF$_4^-$**. (b) Oxo group transfer from **4a$^+$BF$_4^-$** to dimethyl sulfide would also give **2a$^+$BF$_4^-$**. Thus, an analogous reaction was conducted with dimethyl sulfide-d_6. Only the labeled substitution product **2a-d_6^+BF$_4^-$** formed, as assayed by ^{1}H NMR spectrometry.

(14) Schilling, B. E. R.; Hoffman, R.; Faller, J. *J. Am. Chem. Soc.* **1979**, *101*, 592.

(15) Lichtenberger, D. L.; Rai-Chaudhuri, A.; Seidel, M. J.; Gladysz, J. A.; Agbossou, S. K.; Igau, A.; Winter, C. H. *Organometallics* **1991**, *10*, 1355.

Table III. Atomic Coordinates and Equivalent Isotropic Thermal Parameters of Non-Hydrogen Atoms in 2a⁺TfO⁻•CH₂Cl₂, 4a⁺BF₄⁻, and 6a⁺TfO⁻ [a]

	x	y	z	B, Å²		x	y	z	B, Å²
				2a⁺TfO⁻·CH₂Cl₂					
Re	0.93126 (4)	0.79676 (1)	0.91968 (2)	2.763 (6)	C17	0.630 (1)	0.8887 (4)	0.6668 (7)	4.8 (2)
P	0.7877 (3)	0.86644 (9)	0.8545 (2)	2.89 (4)	C18	0.653 (1)	0.8930 (4)	0.9387 (6)	3.4 (2)
N	0.7535 (9)	0.7760 (3)	0.9682 (5)	3.9 (2)	C19	0.690 (1)	0.8860 (4)	1.0387 (6)	4.2 (2)
O1	0.6440 (9)	0.7645 (3)	1.0081 (6)	6.8 (2)	C20	0.593 (1)	0.9072 (4)	1.1023 (7)	4.5 (2)
S1	0.8654 (3)	0.7519 (1)	0.7712 (2)	4.16 (5)	C21	0.456 (1)	0.9338 (4)	1.0681 (8)	5.1 (2)
C1	1.098 (1)	0.7964 (4)	1.0598 (7)	5.0 (3)	C22	0.419 (1)	0.9401 (4)	0.9683 (8)	4.6 (2)
C2	1.147 (1)	0.7583 (4)	1.0048 (8)	4.9 (2)	C23	0.522 (1)	0.9198 (4)	0.9044 (7)	4.3 (2)
C3	1.208 (1)	0.7789 (4)	0.9223 (7)	4.2 (2)	C24	0.970 (2)	0.6938 (5)	0.781 (1)	7.9 (4)
C4	1.191 (1)	0.8274 (5)	0.9255 (8)	4.8 (2)	C25	0.964 (2)	0.7790 (6)	0.6734 (8)	8.4 (3)
C5	1.117 (1)	0.8421 (5)	1.0126 (8)	5.7 (3)	C26	0.389 (1)	0.6278 (5)	0.9059 (8)	6.3 (3)
C6	0.916 (1)	0.9174 (4)	0.8239 (6)	3.6 (2)	C27	0.723 (2)	1.0405 (6)	0.633 (1)	7.3 (4)
C7	0.911 (1)	0.9624 (4)	0.8729 (8)	4.4 (2)	F1	0.459 (1)	0.5912 (4)	0.9454 (7)	11.3 (3)
C8	1.014 (2)	1.0000 (4)	0.843 (1)	7.0 (3)	F2	0.353 (1)	0.6579 (4)	0.9727 (6)	10.0 (3)
C9	1.114 (1)	0.9944 (5)	0.772 (1)	7.2 (3)	F3	0.241 (1)	0.6143 (5)	0.8708 (8)	14.2 (3)
C10	1.116 (2)	0.9512 (5)	0.7271 (9)	6.8 (3)	S2	0.4929 (3)	0.6566 (1)	0.8134 (2)	4.31 (5)
C11	1.021 (1)	0.9112 (4)	0.7538 (8)	5.1 (2)	O2	0.394 (1)	0.6962 (4)	0.7798 (8)	9.0 (3)
C12	0.6417 (9)	0.8574 (4)	0.7450 (6)	3.3 (2)	O3	0.501 (2)	0.6196 (4)	0.7424 (7)	9.7 (3)
C13	0.535 (1)	0.8190 (4)	0.7466 (6)	3.6 (2)	O4	0.650 (1)	0.6660 (6)	0.8649 (9)	11.7 (4)
C14	0.417 (1)	0.8120 (4)	0.6670 (8)	4.4 (2)	Cl1	0.7634 (6)	1.0033 (2)	0.5377 (3)	8.3 (1)
C15	0.402 (1)	0.8425 (5)	0.5892 (7)	5.5 (3)	Cl2	0.5459 (6)	1.0276 (2)	0.6800 (3)	10.7 (1)
C16	0.509 (2)	0.8813 (5)	0.5873 (8)	6.0 (3)					
				4a⁺BF₄⁻					
Re	0.22470 (3)	0.35174 (2)	0.24523 (3)	3.772 (6)	C13	0.5351 (8)	0.0983 (6)	0.2683 (8)	4.9 (2)
S	0.3518 (2)	0.4449 (1)	0.1266 (2)	4.17 (4)	C14	0.6484 (9)	0.0837 (7)	0.3387 (9)	5.9 (2)
P	0.3505 (2)	0.2089 (1)	0.1471 (2)	3.61 (4)	C15	0.7261 (9)	0.1600 (8)	0.3862 (9)	6.5 (2)
O1	0.3690 (7)	0.4026 (6)	0.5169 (7)	8.7 (2)	C16	0.6914 (8)	0.2504 (7)	0.363 (1)	6.3 (2)
O2	0.4767 (5)	0.4050 (4)	0.0733 (6)	5.2 (1)	C17	0.5777 (8)	0.2650 (6)	0.2918 (9)	5.3 (2)
N	0.3156 (6)	0.3807 (5)	0.4020 (8)	5.5 (2)	C18	0.3983 (7)	0.1967 (5)	-0.0410 (7)	3.8 (2)
C1	0.0409 (9)	0.4358 (6)	0.233 (1)	6.1 (2)	C19	0.5246 (8)	0.1753 (6)	-0.0831 (8)	4.9 (2)
C2	0.0333 (9)	0.3901 (7)	0.348 (1)	6.7 (2)	C20	0.5557 (8)	0.1723 (6)	-0.2278 (9)	5.8 (2)
C3	0.0373 (8)	0.2880 (7)	0.296 (1)	6.1 (2)	C21	0.4649 (9)	0.1912 (7)	-0.3245 (9)	6.1 (2)
C4	0.0437 (7)	0.2750 (6)	0.1450 (9)	5.3 (2)	C22	0.3406 (9)	0.2114 (7)	-0.2839 (8)	6.1 (2)
C5	0.0446 (8)	0.3639 (6)	0.1066 (9)	5.4 (2)	C23	0.3056 (8)	0.2152 (6)	-0.1411 (8)	4.9 (2)
C6	0.2616 (7)	0.1015 (5)	0.1519 (8)	4.2 (2)	C24	0.3793 (9)	0.5564 (6)	0.242 (1)	6.1 (2)
C7	0.2362 (8)	0.0335 (6)	0.0305 (9)	5.2 (2)	C25	0.2681 (9)	0.4869 (7)	-0.0167 (9)	6.5 (2)
C8	0.163 (1)	-0.0444 (7)	0.040 (1)	7.5 (3)	B	0.026 (1)	0.7114 (8)	0.311 (1)	6.4 (3)
C9	0.117 (1)	-0.0552 (7)	0.170 (1)	8.4 (3)	F1	0.1083 (6)	0.6622 (5)	0.3864 (7)	9.2 (2)
C10	0.143 (1)	0.0101 (7)	0.292 (1)	7.7 (2)	F2	-0.0079 (7)	0.7975 (4)	0.3934 (7)	9.5 (2)
C11	0.2150 (9)	0.0896 (6)	0.2860 (9)	6.0 (2)	F3	-0.0761 (6)	0.6556 (5)	0.2762 (9)	11.0 (2)
C12	0.4980 (7)	0.1897 (6)	0.2444 (7)	4.1 (2)	F4	0.082 (1)	0.7201 (6)	0.1903 (8)	16.4 (3)
				6a⁺TfO⁻					
Re	0.30259 (7)	0.17426 (2)	0.00627 (8)	3.72 (1)	C7	0.144 (4)	0.0655 (9)	0.172 (4)	13.6 (9)
S1	0.3163 (6)	0.0820 (2)	0.0730 (7)	6.3 (1)	C8	0.281 (3)	0.0430 (8)	-0.125 (4)	9.2 (7)
O1	-0.031 (1)	0.1937 (6)	0.089 (2)	7.8 (4)	C9*	-0.243 (1)	0.065 (2)	-0.515 (1)	13.3 (1)
O2	0.222 (2)	0.1615 (6)	-0.408 (2)	8.3 (4)	F1*	-0.140 (3)	0.0343 (8)	-0.485 (2)	17.7 (6)
N	0.100 (2)	0.1825 (5)	0.052 (2)	5.0 (3)	F2*	-0.217 (2)	0.0936 (7)	-0.629 (2)	17.0 (6)
C1	0.574 (2)	0.1789 (7)	0.084 (3)	5.5 (4)	F3*	-0.381 (4)	0.045 (1)	-0.547 (4)	16.5 (1)
C2	0.535 (2)	0.2159 (7)	-0.043 (3)	5.4 (4)	S2	-0.2544 (7)	0.1037 (2)	-0.3016 (7)	6.3 (1)
C3	0.429 (2)	0.2532 (6)	0.016 (3)	6.2 (5)	O3*	-0.289 (3)	0.0695 (6)	-0.165 (2)	12.1 (6)
C4	0.403 (2)	0.2384 (7)	0.205 (3)	7.2 (5)	O4*	-0.363 (3)	0.1407 (7)	-0.354 (2)	15.1 (6)
C5	0.500 (2)	0.1927 (8)	0.243 (2)	6.7 (5)	O5*	-0.092 (3)	0.120 (1)	-0.272 (4)	14.0 (1)
C6	0.251 (2)	0.1630 (7)	-0.252 (2)	4.9 (4)					

[a] B values for atoms refined anisotropically are given in the form of the isotropic equivalent displacement parameter defined as $\frac{4}{3}[a^2B_{11} + b^2B_{22} + c^2B_{33} + ab(\cos \gamma)B_{12} + ac(\cos \beta)B_{13} + bc(\cos \alpha)B_{23}]$. Atoms refined isotropically are starred.

complex (η^5-C₅H₅)Re(NO)(CO)(OTf) (5, 72%; Scheme III). Subsequent reaction of 5 with dimethyl sulfide (a) and bis(*tert*-butyl) sulfide (e) gave complexes [(η^5-C₅H₅)Re-(NO)(CO)(SR₂)]⁺TfO⁻ (6a,e⁺TfO⁻) in 99–81% yields after workup.

Complexes 6a,e⁺TfO⁻ were characterized in a manner identical with that for 2⁺TfO⁻ (Table I). Complex 6a⁺TfO⁻ exhibited one ¹H and ¹³C NMR resonance for the two diastereotopic methyl groups at room temperature. Similarly, 6e⁺TfO⁻ exhibited one set of ¹H and ¹³C NMR resonances for the diastereotopic *tert*-butyl groups. Low-temperature NMR experiments are described below.

A crystal structure of 6a⁺TfO⁻ (Figure 3) was executed analogously to that of 2a⁺TfO⁻ above. Structural data are summarized in Tables III and IV. The nitrosyl and carbonyl ligands were distinguished on the basis of bond length trends (Re–CO > Re–NO) previously found in rhenium carbonyl nitrosyl complexes.[17]

5. Dynamic NMR Studies. Variable-temperature ¹H and ¹³C{¹H} NMR spectra of dimethyl sulfide complexes 2a⁺TfO⁻ and 6a⁺TfO⁻ were recorded in CD₂Cl₂. Those of 2a⁺TfO⁻ are representative and are illustrated in Figure 4. Additional spectra are shown elsewhere.[11] In both compounds, separate resonances were observed for the

(16) (a) Casey, C. P.; Andrews, M. A.; McAlister, D. R.; Rinz, J. E. *J. Am. Chem. Soc.* **1980**, *102*, 1927. (b) Sweet, J. R.; Graham, W. A. G. *Ibid.* **1982**, *104*, 2811.

(17) For example, Re–CO and Re–NO bond lengths of 2.00 and 1.80 Å are found in (η^1-C₅H₅)Re(PMe₃)₂(NO)(CO)(CH₃): Casey, C. P.; O'-Connor, J. M.; Jones, W. D.; Haller, K. J. *Organometallics* **1983**, *2*, 535.

Table IV. Selected Bond Lengths (Å), Bond Angles (deg), and Torsion Angles (deg) in 2a⁺TfO⁻•CH₂Cl₂, 4a⁺BF₄⁻, and 6a⁺TfO⁻ [a,b]

2a⁺TfO⁻·CH₂Cl₂			
Re–S1	2.395 (3)	Re–C4	2.29 (1)
Re–P	2.370 (2)	Re–C5	2.26 (1)
Re–N	1.775 (8)	S1–C24	1.81 (1)
N–O	1.16 (1)	S1–C25	1.81 (1)
Re–C1	2.24 (1)	P–C6	1.83 (1)
Re–C2	2.27 (1)	P–C12	1.835 (8)
Re–C3	2.336 (9)	P–C18	1.849 (9)
S1–Re–P	92.10 (8)	C1–C2–C3	107 (1)
S1–Re–N	92.4 (3)	C2–C3–C4	109 (1)
P–Re–N	90.2 (3)	C3–C4–C5	111 (1)
Re–S1–C24	109.5 (5)	C4–C5–C1	102 (1)
Re–S1–C25	110.4 (5)	C5–C1–C2	111 (1)
C24–S1–C25	99.4 (7)		
P–Re–S1–LP	–59.3 (2)	N–Re–S1–LP	30.9 (3)
P–Re–S1–C24	174.7 (5)	N–Re–S1–C24	–95.1 (6)
P–Re–S1–C25	66.2 (5)	N–Re–S1–C25	156.5 (6)
4a⁺BF₄⁻			
Re–S	2.349 (1)	Re–C4	2.320 (6)
Re–P	2.407 (1)	Re–C5	2.299 (6)
Re–N	1.738 (6)	S–C24	1.770 (7)
N–O1	1.205 (7)	S–C25	1.783 (7)
S–O2	1.462 (4)	P–C6	1.823 (6)
Re–C1	2.238 (7)	P–C12	1.824 (6)
Re–C2	2.242 (7)	P–C18	1.827 (5)
Re–C3	2.287 (6)		
S–Re–P	90.74 (5)	O2–S–C25	108.3 (3)
S–Re–N	91.1 (2)	C1–C2–C3	109.0 (7)
P–Re–N	95.1 (2)	C2–C3–C4	105.9 (7)
Re–S–C24	109.5 (2)	C3–C4–C5	108.7 (6)
Re–S–C25	112.5 (2)	C4–C5–C1	109.1 (6)
C24–S–C25	99.7 (4)	C5–C1–C2	107.2 (6)
O2–S–C24	106.6 (3)		
P–Re–S–O2	–17.2 (3)	N–Re–S–O2	77.9 (4)
P–Re–S–C24	–139.7 (3)	N–Re–S–C24	–44.6 (4)
P–Re–S–C25	110.4 (3)	N–Re–S–C25	–154.5 (4)
6a⁺TfO⁻			
Re–S1	2.391 (3)	Re–C2	2.278 (9)
Re–N	1.773 (9)	Re–C3	2.260 (9)
N–O	1.20 (1)	Re–C4	2.27 (1)
Re–C6	1.90 (1)	Re–C5	2.288 (9)
C6–O1	1.14 (1)	S1–C7	1.73 (2)
Re–C1	2.274 (9)	S1–C8	1.75 (1)
S1–Re–C6	93.1 (3)	C1–C2–C3	112 (1)
S1–Re–N	95.8 (2)	C2–C3–C4	107 (1)
N–Re–C6	95.4 (3)	C3–C4–C5	104 (1)
Re–S1–C7	107.5 (5)	C4–C5–C1	109 (1)
Re–S1–C8	112.8 (5)	C5–C1–C2	107 (1)
C7–S1–C8	98.2 (8)		
C6–Re–S1–LP	130.0 (6)	N–Re–S1–LP	–134.3 (5)
C6–Re–S1–C7	–105.8 (11)	N–Re–S1–C7	–10.0 (11)
C6–Re–S1–C8	1.4 (10)	N–Re–S1–C8	97.1 (10)

[a] Bond lengths and angles involving the phenyl rings have been omitted. [b] LP = lone pair.

diastereotopic methyl groups at low temperatures. The resonances coalesced when the samples were warmed. Thus, some dynamic process can render the two methyl groups equivalent.

Application of the coalescence formula[18] gave $\Delta G^{*}(T_c)$ for the process rendering the methyl groups equivalent as 9.6–9.8 kcal/mol for 2a⁺TfO⁻ and 12.6–12.9 kcal/mol for 6a⁺TfO⁻. Data are summarized in Table V. Similarly, low-temperature ¹³C NMR spectra of bis(*tert*-butyl) sulfide complex 6e⁺BF₄⁻ showed two *tert*-butyl C(CH₃)₃ and C-

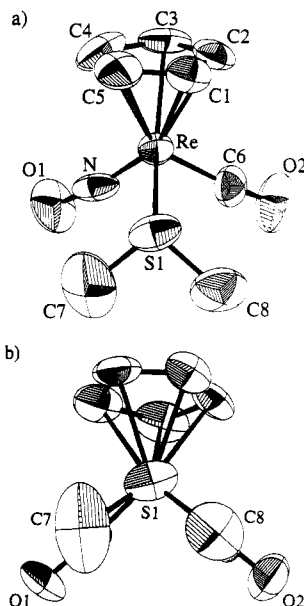(18) Sandström, J. *Dynamic NMR Spectroscopy*; Academic Press: New York, 1982; Chapter 7.

Figure 3. Structure of the cation of dimethyl sulfide complex [(η⁵-C₅H₅)Re(NO)(CO)(SMe₂)]⁺TfO⁻ (6a⁺TfO⁻): (a) numbering diagram; (b) Newman-type projection.
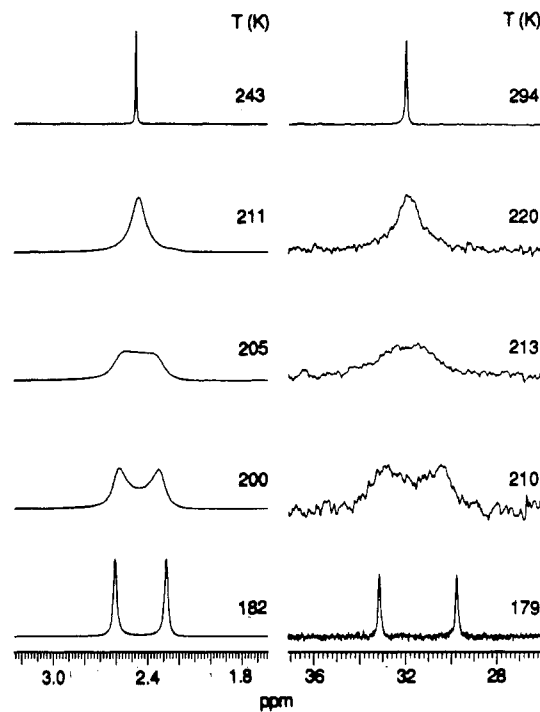
Figure 4. Variable-temperature ¹H and ¹³C{¹H} NMR spectra of 2a⁺TfO⁻ (CD₂Cl₂, methyl group region).

Table V. Summary of Dynamic ¹H and ¹³C{¹H} NMR Data [a]

compd	resonance	T_c,[b] K	δ_ν,[c] Hz	$\Delta G^{\ddagger}(T_c)$,[d] kcal/mol
2a⁺TfO⁻	SCH₃	205	98	9.7
	SCH₃	213	254	9.6
6a⁺TfO⁻	SCH₃	263	49	12.9
	SCH₃	260	61	12.6
6e⁺TfO⁻	CH₃	<178		
	C(CH₃)₃	207	191	9.5
	C(CH₃)₃	206	154	9.5

[a] At 300 (¹H) or 75 (¹³C) MHz in CD₂Cl₂. [b] Decoalescence temperature. [c] Frequency difference between resonances of exchanging groups in low-temperature limit (188 K). [d] Error limit estimated as ±0.1 kcal/mol.

(CH$_3$)$_3$ resonances. Coalescence data (Table V) gave $\Delta G^{\ddagger}(T_c)$ of 9.5 kcal/mol. Interestingly, both C(CH$_3$)$_3$ resonances were sharp in the low-temperature limit ($\Delta\nu_{1/2}$ 3.7–3.9 Hz), but one C(CH$_3$)$_3$ resonance was broadened relative to the other ($\Delta\nu_{1/2}$ 31.8, 10.5 Hz).

Additional experiments were conducted to probe the mechanism of alkyl group exchange. First, the methyl ^{13}C NMR resonances of **2a**$^+$TfO$^-$ in Figure 4 did not exhibit carbon–phosphorus coupling ($^3J_{CP}$; $\Delta\nu_{1/2}$ 6.6 Hz, 21 °C). However, a ^{13}C NMR spectrum in CDCl$_3$ (Table I) showed a $^3J_{CP}$ of 2.6 Hz. Second, dimethyl sulfide-d_6 (S(CD$_3$)$_2$, 5 equiv) was added to a sample of **2a**$^+$TfO$^-$ (0.04 M in CD$_2$Cl$_2$) at 35 °C. Before addition, the area ratio of the cyclopentadienyl and methyl ^{1}H NMR resonances was (46 ± 2):(54 ± 2). Eight hours after addition, the ratio remained unchanged. These data require that a process other than simple sulfide ligand dissociation must be responsible for the dynamic NMR behavior in Figure 4.

Low-temperature ^{1}H NMR spectra of unsymmetrical sulfide complexes **2b,c**$^+$TfO$^-$ were recorded in CD$_2$Cl$_2$. In each case, two diastereomers, differing in the relative configurations at rhenium and sulfur, decoalesced. Methyl ethyl sulfide complex **2b**$^+$TfO$^-$ gave a (67 ± 2):(33 ± 2) mixture of isomers at –95 °C (δ, major/minor: 5.65/5.62, C$_5$H$_5$; 2.26/2.55, SCH$_3$; 2.74/3.16, SCH$_2$; 1.29/1.03 CH$_2$CH$_3$). Methyl isopropyl sulfide complex **2c**$^+$TfO$^-$ gave a (77 ± 2):(23 ± 2) mixture of isomers at –95 °C (δ, major/minor: 5.64/5.51, C$_5$H$_5$; 2.20/1.92, SCH$_3$). Diastereomer configurations are assigned below.

Discussion

1. Synthesis and Spectroscopic Properties of the New Complexes.
Schemes I and II establish that sulfide complexes **2**$^+$X$^-$ can be accessed from either triflate complex **1** or dichloromethane complex **3**$^+$BF$_4^-$. Amines also displace the triflate ligand from **1**,[19] but substitutions do not proceed to completion with weaker Lewis bases (e.g., bis(*tert*-butyl) sulfide). In contrast, weak Lewis bases such as alkyl iodides[8a] readily displace the dichloromethane ligand from **3**$^+$BF$_4^-$.

The spectroscopic properties of **2**$^+$X$^-$ (Table I) can be compared with those of analogous ether complexes [(η^5-C$_5$H$_5$)Re(NO)(PPh$_3$)(OR$_2$)]$^+$X$^-$ (**7**$^+$X$^-$; R = Me, Et, –CH$_2$CH$_2$–).[8b] First, the IR ν_{NO} values of **2**$^+$X$^-$ are somewhat higher (1716–1700 cm^{-1} vs 1700–1692 cm^{-1}). Similarly, the cyclopentadienyl ^{1}H NMR resonances of **2**$^+$X$^-$ (δ 5.66–5.63, CDCl$_3$) are slightly downfield of those of **7**$^+$X$^-$ (δ 5.63–5.50, CD$_2$Cl$_2$). Also, the PPh$_3$ ligand ^{31}P NMR chemical shifts in **2**$^+$X$^-$ (11.0–11.9 ppm) appear distinctly upfield from those of **7**$^+$X$^-$ (17.4–18.1 ppm). These trends are in accord with the commonly accepted π-acidity order R$_2$S > R$_2$O.[20]

Sulfoxide complexes **4**$^+$BF$_4^-$ can be prepared analogously to **2**$^+$BF$_4^-$. Complex **4a**$^+$BF$_4^-$ exhibits IR ν_{NO} bands and cyclopentadienyl and PPh$_3$ ligand NMR chemical shifts that are close to those of **2a**$^+$TfO$^-$ (Table I). Although differences are small, trends are in accord with the prevailing view that sulfoxides are slightly better π acceptors (and poorer σ donors) than sulfides.[21]

(19) Dewey, M. A.; Bakke, J. M.; Gladysz, J. A. *Organometallics* **1990**, *9*, 1349.

(20) (a) Cotton, F. A.; Wilkinson, G. *Advanced Inorganic Chemistry*, 3rd ed.; Wiley: New York, 1972; p 720. (b) Cotton, F. A. *Inorg. Chem.* **1964**, *3*, 702. (c) Hieber, W.; Opavsky, W.; Rohm, W. *Chem. Ber.* **1968**, *101*, 2244.

(21) (a) Davies, J. A. *Adv. Inorg. Chem. Radiochem.* **1981**, *24*, 115. (b) Kukushkin, Yu. N.; Gur'yanova, G. P. *Russ. J. Inorg. Chem. (Engl. Transl.)* **1971**, *16*, 580. (c) James, B. R.; Pacheco, A.; Rettig, S. J.; Ibers, J. A. *Inorg. Chem.* **1988**, *27*, 2414. (d) Riley, D.; Lyon, J., III. *J. Chem. Soc., Dalton Trans.* **1991**, 157.

The carbonyl-substituted sulfide complexes **6**$^+$TfO$^-$ can be synthesized analogously to **2**$^+$TfO$^-$. However, they exhibit ν_{NO} values that are considerably higher (1738–1746 cm^{-1}). This can be attributed to the poorer π basicity of the carbonyl-substituted rhenium fragment [(η^5-C$_5$H$_5$)-Re(NO)(CO)]$^+$ (**II**).[14,15] In this context, the frontier molecular orbitals of **I**, **II**, and related metal fragments have been studied in detail.[14,15] The highest occupied orbitals of **I** and **II** are shown in Scheme IV. The relative orbital energies of these orbitals are largely determined by the π-acidity strength of the ligands they can back-bond to (PPh$_3$ < CO < NO). Thus, **Ia** is considerably higher in energy than **IIa**, and the energy difference between **Ia** and **Ib** is greater than that between **IIa** and **IIb**.

2. Basic Structural Features of Sulfide and Sulfoxide Complexes.
Complexes **2a**$^+$TfO$^-$, **4a**$^+$BF$_4^-$, and **6a**$^+$TfO$^-$ belong to a large class of formally octahedral complexes in which the cyclopentadienyl ligand occupies three coordination sites.[22] Thus, S–Re–N, S–Re–P (or S–Re–CO), and N–Re–P (or N–Re–CO) bond angles of ca. 90° are found (Table IV).

Uncoordinated dimethyl sulfide exhibits a carbon–sulfur bond length of 1.802 (2) Å and a C–S–C angle of 98.52 (10)°.[23] The coordinated dimethyl sulfide in **2a**$^+$TfO$^-$ exhibits very similar bond lengths and angles. However, the carbon–sulfur bonds in **6a**$^+$TfO$^-$ (1.73 (2)–1.75 (1) Å) appear slightly contracted.

Uncoordinated dimethyl sulfoxide exhibits carbon–sulfur and sulfur–oxygen bond lengths of 1.798 (10) and 1.531 (5) Å and C–S–C and C–S–O angles of 97.4 (4) and 106.7 (4)°.[12a,21a,24] Complex **4a**$^+$BF$_4^-$ exhibits similar bond angles and carbon–sulfur bond lengths. However, the sulfur–oxygen bond (1.462 (4) Å) is slightly shorter. Sulfur–oxygen bond lengths in other metal DMSO complexes range from 1.45 to 1.51 Å, with an average of ca. 1.47 Å.[21a,25]

The rhenium–sulfur bond length in **2a**$^+$TfO$^-$ (2.395 (3) Å) is very close to that of **6a**$^+$TfO$^-$ but longer than that in **4a**$^+$BF$_4^-$ (2.349 (1) Å). Thus, the stronger π-accepting ligand gives the shorter rhenium–sulfur bond. However, repulsive interactions between occupied rhenium orbitals

(22) Caulton, K. G. *Coord. Chem. Rev.* **1981**, *38*, 1.

(23) Pierce, L.; Hayashi, M. *J. Chem. Phys.* **1961**, *35*, 479.

(24) Thomas, R.; Shoemaker, C. B.; Eriks, K. *Acta Crystallogr.* **1966**, *21*, 12.

(25) Belsky, V. K.; Konovalov, V. E.; Kukushkin, V. Yu.; Moiseev, A. I. *Inorg. Chim. Acta* **1990**, *169*, 101.

Scheme V. Mechanism for Exchange of the Diastereotopic Methyl Groups in Dimethyl Sulfide Complex $[(\eta^5\text{-}C_5H_5)Re(NO)(PPh_3)(SMe_2)]^+X^-$ (2a$^+$X$^-$)

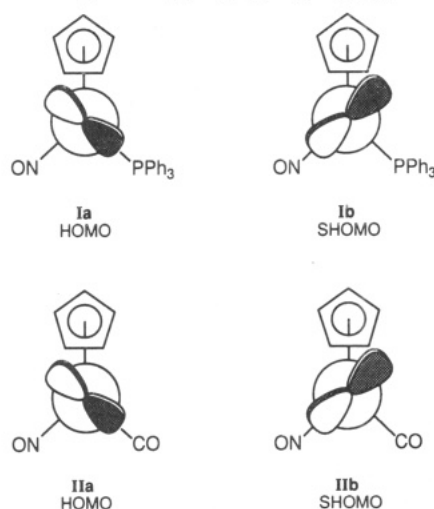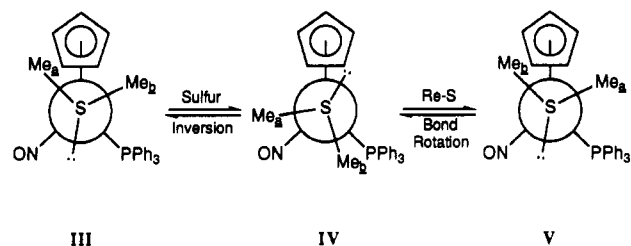III   IV   V

(Scheme IV) and the sulfur lone pairs in 2a$^+$TfO$^-$ and 6a$^+$TfO$^-$ (discussed below) may also contribute to this difference.

Crystal structures of other rhenium sulfide complexes have been previously reported.[26-28] However, most of those with rhenium in a lower oxidation state contain a macrocyclic sulfide ligand and, thus, are not good models for 2a$^+$TfO$^-$ and 6a$^+$TfO$^-$. A novel bridging thiophene complex with a $(\eta^5\text{-}C_5Me_5)Re(CO)_2(SR_2)$ linkage has been described by Angelici.[27] Also, the crystal structure of the iron dimethyl sulfide complex $[(\eta^5\text{-}C_5H_5)Fe(CO)_2(SMe_2)]^+BF_4^-$, which is "isoelectronic" with 6a$^+$TfO$^-$, has been determined.[29] The metal–sulfur bond (2.264 (2) Å) is 5% shorter than that of 6a$^+$TfO$^-$—a contraction typical of analogous first- and third-row metal complexes.

3. Configurational Properties of Sulfide Ligands. The exchange of the diastereotopic sulfur substituents in 2a$^+$TfO$^-$ and 6a,e$^+$TfO$^-$ (Figure 4 and Table V) does not entail sulfide ligand dissociation. Therefore, two distinct intramolecular events are required, as illustrated in Scheme V.[30] First, the sulfur atom must invert. Second, the rhenium–sulfur bond must rotate to return the alkyl groups to their original positions. Thus, the barriers in Table V constitute *upper limits* to the sulfur inversion barriers.

It is instructive to compare the barriers in the carbonyl-substituted complexes 6a,e$^+$TfO$^-$. Pyramidal atoms commonly distort toward a planar geometry when bulky groups are attached.[31] Consequently, inversion barriers are lowered. Accordingly, $\Delta G^\ddagger$ is less for *tert*-butyl-substituted sulfide complex 6e$^+$TfO$^-$ than methyl-substituted sulfide complex 6a$^+$TfO$^-$. However, if rhenium–sulfur bond rotation were rate determining in Scheme V, a *higher* barrier would have been predicted for 6e$^+$TfO$^-$.

Similarly, $\Delta G^\ddagger$ for methyl group exchange in 2a$^+$TfO$^-$ is lower than that in 6a$^+$TfO$^-$. Since the rhenium fragment in the former complex is much bulkier, the opposite order would be expected if rhenium–sulfur bond rotation were rate determining. Thus, the $\Delta G^\ddagger$ values in Table V likely

	$\Delta G^\ddagger$ (298 K, kcal/mol)		$\Delta G^\ddagger$ (T_c, kcal/mol)
R = **a**, *t*-butyl	10.1	E = **a**, P	12.9
b, *i*-propyl	11.3	**b**, As	12.8
c, ethyl	12.4	**c**, Sb	12.4
d, methyl	12.8		

Figure 5. Sulfur inversion barriers of selected sulfide complexes.

10   VI

R = **d**, *t*-Bu	10d :	∠ P1-Re-P2-LP	58.9°
f, Ph		∠ P1-Re-P2-R$_a$	171.6°
		∠ P1-Re-P2-R$_b$	64.8°
		∠ N-Re-P2-R$_a$	80.6°
		∠ N-Re-P2-R$_b$	157.3°
	10f :	∠ P1-Re-P2-LP	59.7°
		∠ P1-Re-P2-R$_a$	175.9°
		∠ P1-Re-P2-R$_b$	62.6°
		∠ N-Re-P2-R$_a$	92.4°
		∠ N-Re-P2-R$_b$	154.3°

Figure 6. Structures of phosphido complexes $(\eta^5\text{-}C_5H_5)Re(NO)(PPh_3)(PR_2)$ (10).

closely approximate the sulfur inversion barriers.

The pyramidal character of the sulfur atoms in 2a$^+$TfO$^-$ and 6a$^+$TfO$^-$ can be compared by summing the Re–S–C, Re–S–C', and C–S–C' bond angles. These quantities (319.3 and 318.5°) are identical within experimental error. Trigonal-planar and idealized tetrahedral sulfur atoms would give values of 360 and 328.5°, respectively. Thus, despite the low inversion barriers, 2a$^+$TfO$^-$ and 6a$^+$TfO$^-$ exhibit considerable pyramidal character.

Inversion barriers for sulfonium salts RR'R"S$^+$X$^-$ are typically 25–32 kcal/mol[2a,32,33]—much higher than those in Table V. Accordingly, crystal structures show somewhat more pyramidal character.[33] However, low inversion/rotation barriers have previously been found for a variety of metal sulfide complexes.[2,34,35] In particular, Abel and co-workers have carefully studied and interpreted the configurational properties of a large number of compounds.[2]

For example, sulfur inversion barriers in the tungsten

(26) (a) Louie, B. M.; Rettig, S. J.; Storr, A.; Trotter, J. *Can. J. Chem.* **1985**, *63*, 2261. (b) Nicholson, T.; Zubieta, J. *Inorg. Chem.* **1987**, *26*, 2094. (c) Hoffmann, P.; Steinhoff, A.; Mattes, R. *Z. Naturforsch., B: Anorg. Chem., Org. Chem.* **1987**, *42*, 867.

(27) Choi, M.-G.; Angelici, R. J. *J. Am. Chem. Soc.* **1989**, *111*, 8753.

(28) Preliminary crystallographic data have been reported for Re-(O)(Cl)$_3$(OPPh$_3$)(SMe$_2$): Bryan, J. C.; Stenkamp, R. E.; Tulip, T. H.; Mayer, J. M. *Inorg. Chem.* **1987**, *26*, 2283.

(29) (a) Schumann, H.; Arif, A. M.; Rheingold, A. L.; Janiak, C.; Hoffmann, R.; Kuhn, N. *Inorg. Chem.* **1991**, *30*, 1618. (b) Kuhn, N.; Schumann, H. *J. Organomet. Chem.* **1984**, *276*, 55.

(30) In theory, an inversion of configuration at rhenium could exchange the diastereotopic sulfur substituents. This is unlikely to be a low-activation-energy pathway, as optically active phosphine complexes $[(\eta^5\text{-}C_5H_5)Re(NO)(PPh_3)(PR_2H)]^+$ and phosphido complexes $(\eta^5\text{-}C_5H_5)$-Re(NO)(PPh$_3$)(PR$_2$) both exhibit excellent configurational stability at room temperature.[31]

(31) (a) Buhro, W. E.; Zwick, B. D.; Georgiou, S.; Hutchinson, J. P.; Gladysz, J. A. *J. Am. Chem. Soc.* **1988**, *110*, 2427. (b) Zwick, B. D.; Arif, A. M.; Patton, A. T.; Gladysz, J. A. *Angew. Chem., Int. Ed. Engl.* **1987**, *26*, 910.
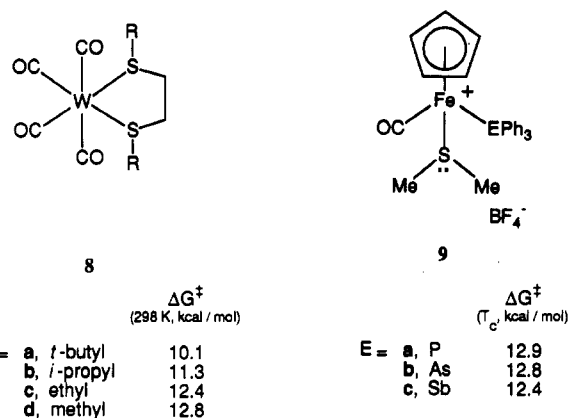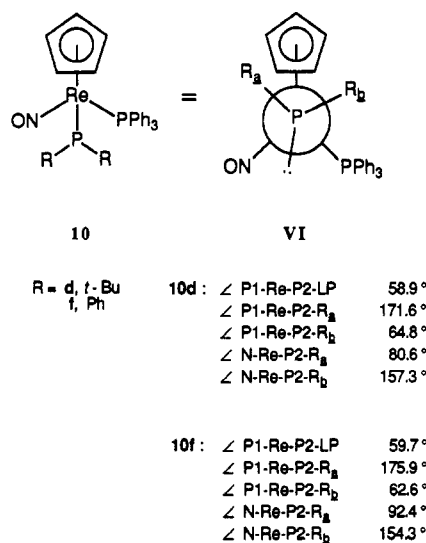
(32) Allen, L. C.; Rauk, A.; Mislow, K. *Angew. Chem., Int. Ed. Engl.* **1970**, *9*, 400.

(33) (a) Roush, D. M.; Price, E. M.; Templeton, L. K.; Templeton, D. H.; Heathcock, C. H. *J. Am. Chem. Soc.* **1979**, *101*, 2971. (b) Farnham, W. B.; Dixon, D. A.; Middleton, W. J.; Calabrese, J. C.; Harlow, R. L.; Whitney, J. F.; Jones, G. A. Guggenberger, L. J. *Ibid.* **1987**, *109*, 476.

(34) (a) Abel, E. W.; Bhatti, M. M.; Orell, K. G.; Sik, V. *J. Organomet. Chem.* **1981**, *208*. 195. (b) See also Abel, E. W.; Corben, R.; Moss, I.; Orrell, K. G.; Richardson, N. R.; Sik, V. *Ibid.* **1988**, *344*, 343.

(35) (a) Kuhn, N.; Schumann, H.; Zauder, E. *J. Organomet. Chem.* **1988**, *327*, 17. (b) Kuhn, N.; Schumann, H. *Inorg. Chim. Acta.* **1986**, *116*, L11.
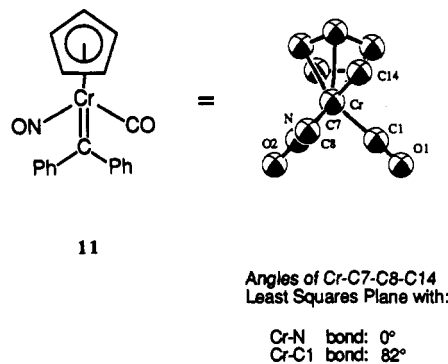
11

Angles of Cr-C7-C8-C14
Least Squares Plane with:

Cr-N bond: 0°
Cr-C1 bond: 82°

Figure 7. Structure of carbene complex $(\eta^5\text{-}C_5H_5)Cr(NO)\text{-}(CO)(=CPh_2)$ **(11)**.

chelate complexes $cis\text{-}W(CO)_4(RSCH_2CH_2SR)$ **(8)** increase regularly in the series R = *tert*-butyl, isopropyl, ethyl, and methyl, as summarized in Figure 5.[2b] The rhenium dimethyl sulfide complex $fac\text{-}Re(CO)_3(Cl)(SMe_2)_2$ exhibits a sulfur inversion barrier $(\Delta G^{\ddagger}(212.5\ K))$ of 11.5 kcal/mol.[34] Inversion barriers have also been measured for several iron dimethyl sulfide complexes $[(\eta^5\text{-}C_5H_5)Fe\text{-}(CO)(EPh_3)(SMe_2)]^+BF_4^-$ **(9)**, as shown in Figure 5.[35] The $\Delta G^{\ddagger}(T_c)$ value found for $2a^+TfO^-$ is ca. 3 kcal/mol less than that of the iron analogue **9a**.

4. Conformational Properties of Sulfide and Sulfoxide Ligands. The sulfide ligand in crystalline $2a^+TfO^-$ adopts a Re–SR_2 bond conformation (Figure 1) very similar to Re–PR_2 conformations previously found in phosphido complexes $(\eta^5\text{-}C_5H_5)Re(NO)(PPh_3)(PR_2)$ **(10;** Figure 6).[31a] The P–Re–P–R and N–Re–P–R torsion angles summarized in Figure 6 are very close to the analogous torsion angles in Table III.

We have previously attributed the Re–PR_2 bond conformations in phosphido complexes **10** to a combination of electronic and steric effects.[31a] For example, there is a potential repulsive interaction between HOMO Ia and the phosphorus lone pair.[36] Accordingly, overlap is minimal in the Re–PR_2 conformations shown in Figure 6. However, note that the rhenium ligands define three interstices. The region between the cyclopentadienyl and nitrosyl ligands is larger than that between the cyclopentadienyl and PPh_3 ligands. The latter is in turn larger than the region between the nitrosyl and PPh_3 ligands $(\angle N\text{-}Re\text{-}P \simeq 90°).$[37,38] Thus, the above Re–PR_2 conformations also direct the phosphorus substituents into the largest interstices.

We had hoped that the study of carbonyl-substituted analogues of **10** and $2a^+TfO^-$ would help evaluate the relative importance of these two conformation-influencing effects. The HOMO and SHOMO of the $[(\eta^5\text{-}C_5H_5)Re\text{-}(NO)(CO)]^+$ fragment (IIa, IIb; Scheme IV) are symmetrically disposed with respect to a "steric" mirror plane. Thus, any given ligand conformation has an "isosteric" but electronically differentiated counterpart. Also, electronic effects upon ligand conformations are well established for d^6 metal fragments of the formula $[(\eta^5\text{-}C_5H_5)M(NO)\text{-}(CO)]^{n+}.$ For example, the diphenylcarbene complex $(\eta^5\text{-}C_5H_5)Cr(NO)(CO)(=CPh_2)$ **(11)** exhibits the structure depicted in Figure 7.[39] The Cr=C bond conformation

Scheme VI. Diastereomeric Equilibria in Sulfide and Sulfoxide Complexes
$[(\eta^5\text{-}C_5H_5)Re(NO)(PPh_3)(S(X)R_LR_S)]^+X^-$ **(**R_L = **Large Group,** R_S = **Small Group)**
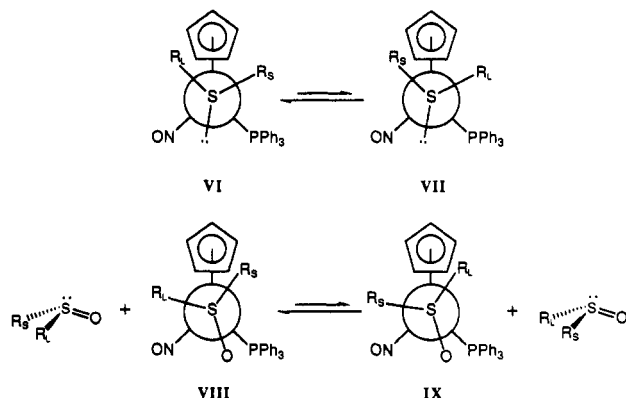
maximizes overlap of the C_α acceptor orbital with the HOMO (which is analogous to IIa)[14] and does not correspond to a steric energy minimum.

However, the conformation of the dimethyl sulfide ligand in crystalline $6a^+TfO^-$ (Figure 3) is fundamentally different from that of the carbene ligand in **11**. The sulfur atom lone pair is symmetrically disposed with respect to HOMO IIa and SHOMO IIb, with overlap angles of ca. 45°. This might be attributable to the closer energy spacing of IIa and IIb and/or to steric effects. Regardless, the *attractive* interaction that is a key determinant of the Cr=C conformation of **11** does not have a *repulsive* counterpart for sulfide ligands in 6^+TfO^-. Still, destabilizing metal/lone-pair interactions *have* been shown to exhibit considerable influence upon the physical and chemical properties of sulfur-containing ligands.[40] Interestingly, the iron dimethyl sulfide complex $[(\eta^5\text{-}C_5H_5)Fe(CO)_2(SMe_2)]^+BF_4^-$ adopts a crystalline M–SMe_2 bond conformation identical with that of $6a^+TfO^-$.[29]

The Re–S bond conformation in sulfoxide complex $4a^+BF_4^-$ is unusual (Figure 3). The S=O and Re—P bonds are nearly eclipsed, as evidenced by the P–Re–S–O torsion angle of −17.2°. Although this might suggest some type of oxygen–phosphorus attractive interaction, no accompanying structural distortions are evident. With related iron alkyl complexes $(\eta^5\text{-}C_5H_5)Fe(CO)(PPh_3)(R)$, Fe–$C_\alpha$ conformations that similarly direct a non-hydrogen substituent toward the PPh_3 ligand have been considered prohibitively high in energy.[38]

We have previously reported the crystal structure of the secondary alkyl complex $SS,RR\text{-}(\eta^5\text{-}C_5H_5)Re(NO)\text{-}(PPh_3)(CH(CH_2C_6H_5)C_6H_5)$ **(12)**.[41] Since C_α contains two alkyl substituents, **12** may be viewed as a crude model for $4a^+BF_4^-$. The P–Re–C_α–H torsion angle in **12** is 35°, with the hydrogen in the nitrosyl–PPh_3 ligand interstice. Thus, the sulfoxide oxygen in $4a^+BF_4^-$ is closer to the PPh_3 ligand than the C_α hydrogen in **12**.

5. Diastereomer Equilibria. The sulfur lone pairs in unsymmetrical sulfides are enantiotopic. Thus, two diastereomers can form upon complexation to the chiral rhenium fragment I. Accordingly, two diastereomers of

(36) (a) Wolfe, S. *Acc. Chem. Res.* **1972**, *5*, 102. (b) Cowley, A. H.; Mitchell, D. J.; Whangbo, M.-H.; Wolfe, S. *J. Am. Chem. Soc.* **1979**, *101*, 5224.

(37) (a) Georgiou, S.; Gladysz, J. A. *Tetrahedron* **1986**, *42*, 1109. (b) Crocco, G. L.; Lee, K. E.; Gladysz, J. A. *Organometallics* **1990**, *9*, 2819.

(38) (a) Seeman, J. I.; Davies, S. G. *J. Am. Chem. Soc.* **1985**, *107*, 6522. (b) Davies, S. G.; Dordor-Hedgecock, I. M.; Sutton, K. H.; Whittaker, M. *Ibid.* **1987**, *109*, 5711.

(39) Herrmann, W. A.; Hubbard, J. L.; Bernal, I.; Korp, J. D.; Haymore, B. L.; Hillhouse, G. L. *Inorg. Chem.* **1984**, *23*, 2978.

(40) (a) Amaresekera, J.; Rauchfuss, T. B.; Wilson, S. R. *Inorg. Chem.* **1987**, *26*, 3328. (b) Ashby, M. T.; Enemark, J. H.; Lichtenberger, D. L. *Inorg. Chem.* **1988**, *27*, 191. (c) Darensbourg, M. Y.; Bischoff, C. J.; Houliston, S. A.; Pala, M.; Reibenspies, J. *J. Am. Chem. Soc.* **1990**, *112*, 6905. (d) Ashby, M. T. *Comments Inorg. Chem.* **1990**, *10*, 297.

(41) Kiel, W. A.; Lin, G.-Y.; Constable, A. G.; McCormick, F. B.; Strouse, C. E.; Eisenstein, O.; Gladysz, J. A. *J. Am. Chem. Soc.* **1982**, *104*, 4865.

2b,c⁺TfO⁻ can be observed by NMR spectroscopy at low temperatures. However, they readily interconvert by a dynamic process analogous to that shown in Scheme V. On the basis of the Re–S conformation of 2a⁺TfO⁻ and steric considerations described above, diastereomers of the type VI should be considerably more stable than VII (Scheme VI). Similar stability trends have been explicitly demonstrated in rhenium alkyl complexes $(\eta^5\text{-}C_5H_5)\text{Re-}$(NO)(PPh₃)(CHRR′).[37b] Thus, the major diastereomers of 2b,c⁺TfO⁻ are assigned the relative rhenium/sulfur configurations shown in VI (R_L = Et, i-Pr; R_S = Me). Note that the two sulfur alkyl groups in 2c⁺TfO⁻ differ more in size than those in 2b⁺TfO⁻. Accordingly, 2c⁺TfO⁻ gives the higher VI/VII equilibrium ratio.

Unsymmetrical sulfoxides are chiral. Thus, two diastereomers are also possible upon binding to the rhenium fragment I. However, in contrast to the situation for the unsymmetrical sulfide complexes, a low-energy intramolecular pathway for diastereomer interconversion does not exist. Thus, benzyl methyl sulfoxide gives two easily distinguished diastereomers.

Unfortunately, a high degree of diastereoselectivity or "chiral recognition" is not observed upon complexation of benzyl methyl sulfoxide. However, on the basis of the Re–S bond conformation of 4a⁺BF₄⁻ and steric factors detailed above, diastereomers of the type VIII (Scheme VI) should be considerably more stable than IX. Thus, under thermodynamically controlled conditions, it may be possible to preferentially bind one enantiomer of a chiral sulfoxide, as illustrated in Scheme VI.

6. Summary. This study has provided high-yield entries into chiral rhenium sulfide and sulfoxide complexes of the formulas $[(\eta^5\text{-}C_5H_5)\text{Re(NO)}(L)(XRR′)]^+X'^-$. The sulfide ligands exhibit some of the lowest sulfur inversion barriers observed to date. Key structural and conformational features of the sulfide and sulfoxide ligands have been defined. Future papers will detail the reaction chemistry of the sulfur-containing ligands.

Experimental Section

General Methods. General procedures have been recently described.[42] Solvents were purified as follows: chlorobenzene, distilled from CaH₂; ether and THF, distilled from LiAlH₄ and then Na/benzophenone; CH₂Cl₂, distilled from P₂O₅ or CaH₂; CD₂Cl₂, vacuum transferred from CaH₂; CDCl₃, distilled from P₂O₅. Sulfides, dimethyl sulfide-d_6, dimethyl sulfoxide, TfOH,[10b] HBF₄·OEt₂ (Aldrich), and benzyl methyl sulfoxide (Parish) were used without purification.

Preparation of $[(\eta^5\text{-}C_5H_5)\text{Re(NO)}(\text{PPh}_3)(\text{SMe}_2)]^+X^-$ (2a⁺X⁻). A. X⁻ = TfO⁻. A Schlenk flask was charged with $(\eta^5\text{-}C_5H_5)\text{Re(NO)}(\text{PPh}_3)(\text{OTf})$ (1,[10] 0.217 g, 0.313 mmol), CH₂Cl₂ (10 mL), dimethyl sulfide (0.115 mL, 1.57 mmol), and a stir bar. The mixture was stirred for 12 h at room temperature. Solvent was removed under oil pump vacuum to give a dark yellow foam. Then CH₂Cl₂ (5 mL) and ether (50 mL) were sequentially added with stirring. The resulting precipitate was washed with ether (3 × 10 mL)[43] to give 2a⁺TfO⁻ as a bright yellow powder (0.225 g, 0.282 mmol, 91%), mp 119–202 °C dec. Anal. Calcd for C₂₆H₂₆F₃NO₄PReS₂: C, 41.37; H, 3.47; S, 8.50. Found: C, 41.26; H, 3.47; S, 8.58. A sample was dissolved in CH₂Cl₂, and ether was slowly added by vapor diffusion. Bright yellow prisms of 2a⁺TfO⁻·CH₂Cl₂ formed, which were washed with ether (3 × 2 mL),[43] mp 198–200 °C dec. Anal. Calcd for C₂₆H₂₆F₃NO₄PReS₂·CH₂Cl₂: C, 38.62; H, 3.36; S, 7.64; Cl, 8.44. Found (two preparations): C, 38.93/38.76; H, 3.40/3.38; S, 7.78/7.62; Cl, 8.35.

B. X⁻ = BF₄⁻. A Schlenk flask was charged with $(\eta^5\text{-}C_5H_5)$-Re(NO)(PPh₃)(CH₃) (0.326 g, 0.585 mmol),[44] CH₂Cl₂ (5 mL), and a stir bar and was cooled to –80 °C. Then HBF₄·OEt₂ (0.087 mL, 0.642 mmol) and dimethyl sulfide (0.129 mL, 1.75 mmol) were added with stirring. After 30 min, the –80 °C bath was removed and the solution was allowed to warm to room temperature. After 2 h, solvent was removed under oil pump vaccum. The residue was washed with hexane (20 mL). Then CH₂Cl₂ (10 mL) and THF (50 mL) were sequentially added. The mixture was concentrated to ca. 5 mL by rotary evaporation. The resulting yellow precipitate was washed with ether/THF (50:50 v/v, 3 × 10 mL)[43] to give 2a⁺BF₄⁻ (0.260 g, 0.376 mmol, 64%). A sample was dissolved in CH₂Cl₂ and layered with ether. Golden prisms of 2a⁺BF₄⁻·0.5CH₂Cl₂ formed, which were washed with ether (3 × 2 mL),[43] mp 145–154 °C dec. Anal. Calcd for C₂₅H₂₆BF₄NOPReS·0.5CH₂Cl₂: C, 41.67; H, 3.70; S, 4.36; Cl, 4.82. Found: C, 41.47; H, 3.67; S, 4.26; Cl, 4.70.

Preparation of $[(\eta^5\text{-}C_5H_5)\text{Re(NO)}(\text{PPh}_3)(\text{S(Et)Me})]^+$TfO⁻ (2b⁺TfO⁻). Complex 1 (0.599 g, 0.865 mmol), CH₂Cl₂ (20 mL), and ethyl methyl sulfide (0.394 mL, 4.35 mmol) were combined in a procedure analogous to that given for 2a⁺TfO⁻. An identical workup gave 2b⁺TfO⁻ as a yellow powder (0.542 g, 0.705 mmol, 81%). A sample was dissolved in THF and layered with ether. Dark yellow prisms of 2b⁺TfO⁻ formed,[43] mp 152–154 °C dec. Anal. Calcd for C₂₇H₂₈F₃NO₄PReS₂: C, 42.18; H, 3.67. Found: C, 42.06; H, 3.63.

Preparation of $[(\eta^5\text{-}C_5H_5)\text{Re(NO)}(\text{PPh}_3)(\text{S(}i\text{-Pr)Me})]^+$TfO⁻ (2c⁺TfO⁻). Complex 1 (0.104 g, 0.150 mmol), CH₂Cl₂ (10 mL), and isopropyl methyl sulfide (0.085 mL, 0.75 mmol) were combined in a procedure analogous to that given for 2a⁺TfO⁻. An identical workup gave 2c⁺TfO⁻ as a yellow powder (0.099 g, 0.126 mmol, 84%). A sample was dissolved in warm THF and layered with ether. Small yellow needles of 2c⁺TfO⁻ formed,[43] mp 220–221 °C dec. Anal. Calcd for C₂₈H₃₀F₃NO₄PReS₂: C, 42.96; H, 3.86. Found: C, 42.92; H, 3.88.

Preparation of $[(\eta^5\text{-}C_5H_5)\text{Re(NO)}(\text{PPh}_3)(\text{S(}t\text{-Bu)Me})]^+$·TfO⁻ (2d⁺TfO⁻). Complex 1 (0.205 g, 0.296 mmol), CH₂Cl₂ (10 mL), and tert-butyl methyl sulfide (0.190 mL, 1.50 mmol) were combined in a procedure analogous to that given for 2a⁺TfO⁻. An identical workup gave 2d⁺TfO⁻ as a dark orange powder (0.122 g, 0.153 mmol, 51%). A sample was dissolved in CH₂Cl₂, and ether was added by vapor diffusion. Bright orange needles of 2d⁺TfO⁻ slowly formed,[43] mp 202–204 °C dec. Anal. Calcd for C₂₉H₃₂F₃NO₄PReS₂: C, 43.71; H, 4.05. Found: C, 43.38; H, 3.94.

Preparation of $(\eta^5\text{-}C_5H_5)\text{Re(NO)}(\text{CO})(\text{OTf})$ (5). A Schlenk flask was charged with $(\eta^5\text{-}C_5H_5)\text{Re(NO)}(\text{CO})(\text{CH}_3)$ (4,[16] 1.000 g, 3.08 mmol), CH₂Cl₂ (20 mL), and a stir bar and was cooled to 0 °C. Then TfOH (0.280 mL, 3.16 mmol)[10b] was added with stirring. After 0.5 h, hexane (20 mL) was added, and solvent was removed under oil pump vacuum. The resulting dark semisolid residue was washed with hexane (3 × 20 mL). The yellow hexane washings were discarded, and the residue was dissolved in CH₂Cl₂ (10 mL). This solution was filtered through silica. Hexane (40 mL) was added to the orange filtrate, and the solution was concentrated by rotary evaporation. Complex 5 precipitated as bright orange microcrystals (1.043 g, 2.275 mmol, 72%),[43] mp 98–99 °C. IR (cm⁻¹, KBr): ν_{NO} 1763 vs, ν_{CO} 2013 vs. ¹H NMR (δ, CDCl₃): 5.95 (s). ¹³C NMR (ppm, CDCl₃): 194.9 (s, CO), 117.5 (q, J_{CF} = 318.7 Hz, CF₃), 93.2 (s, C₅H₅). ¹⁹F NMR (ppm, CDCl₃; C₆F₆ standard): 91.1 (s). Anal. Calcd for C₇H₅F₃NO₅ReS₂: C, 18.34; H, 1.10; S, 6.99. Found: C, 18.22; H, 1.34; S, 6.89.

Preparation of $[(\eta^5\text{-}C_5H_5)\text{Re(NO)}(\text{CO})(\text{SMe}_2)]^+$TfO⁻ (6a⁺TfO⁻). Complex 5 (1.40 g, 3.05 mmol), CH₂Cl₂ (25 mL), and dimethyl sulfide (0.650 mL, 8.85 mmol) were combined in a procedure analogous to that given for 2a⁺TfO⁻. The solution was stirred for 12 h. Solvent was then removed under oil pump vacuum. The resulting yellow powder was washed with ether (3 × 10 mL) to give 6a⁺TfO⁻ (1.58 g, 3.03 mmol, >99%),[43] mp 100–104 °C dec. Anal. Calcd for C₉H₁₁F₃NO₅ReS₂: C, 20.77; H, 2.13; S, 12.32. Found: C, 20.88; H, 2.15; S, 12.38.

Preparation of $[(\eta^5\text{-}C_5H_5)\text{Re(NO)}(\text{CO})(\text{S(}t\text{-Bu)}_2)]^+$TfO⁻ (6e⁺TfO⁻). Complex 5 (0.200 g, 0.436 mmol), CH₂Cl₂ (10 mL), and bis(tert-butyl) sulfide (0.396 mL, 2.20 mmol) were combined

(42) Agbossou, S. K.; Bodner, G. S.; Patton, A. T.; Gladysz, J. A. *Organometallics* 1990, 9, 1184.

(43) The sample was collected by filtration and dried under oil pump vacuum.

(44) Tam, W.; Lin, G.-Y.; Wong, W.-K.; Kiel, W. A.; Wong, V. K.; Gladysz, J. A. *J. Am. Chem. Soc.* 1982, 104, 141.

in a procedure analogous to that given for 2a⁺TfO⁻. The solution was stirred for 6 h. Solvent was then removed under oil pump vacuum to give a dark yellow semisolid. Then THF (5 mL) and ether (50 mL) were sequentially added with stirring. This gave **6e** (0.204 g, 0.353 mmol, 81%) as a bright yellow powder. A sample was dissolved in THF and layered with ether. This gave bright yellow polymorphic plates of 6e⁺TfO⁻,[43] mp 104–105 °C dec. Anal. Calcd for $C_{15}H_{23}F_3NO_5ReS_2$: C, 29.80; H, 3.83; S, 10.60. Found: C, 29.88; H, 3.82; S, 10.52.

Preparation of [(η⁵-C₅H₅)Re(NO)(PPh₃)(S(=O)Me₂)]⁺BF₄⁻ (4a⁺BF₄⁻). Methyl complex (η⁵-C₅H₅)Re(NO)(PPh₃)(CH₃) (0.312 g, 0.558 mmol), CH₂Cl₂ (5 mL), HBF₄·OEt₂ (0.083 mL, 0.614 mmol), and dimethyl sulfoxide (0.119 mL, 1.67 mmol) were combined in a procedure analogous to that given for 2a⁺BF₄⁻. After 30 min, the –80 °C bath was removed and the solution allowed to warm to room temperature. After 2 h, ether (20 mL) was added. The resulting yellow precipitate was washed with ether (3 × 10 mL)[43] to give 4a⁺BF₄⁻ (0.339 g, 0.478 mmol, 86%). A sample was dissolved in CH₂Cl₂ and layered with ether. Bronze prisms of 4a⁺BF₄⁻ formed, which were washed with ether (3 × 2 mL),[43] mp 153–156 °C dec. Anal. Calcd for $C_{25}H_{26}BF_4NO_2PReS$: C, 42.38; H, 3.70; S, 4.52. Found: C, 42.44; H, 3.73; S, 4.59.

Reaction of 4a⁺BF₄⁻ and SMe₂. A Schlenk flask was charged with 4a⁺BF₄⁻ (0.049 g, 0.069 mmol), chlorobenzene (4 mL), and a stir bar. The flask was warmed to 65 °C, and dimethyl sulfide (0.151 mL, 2.06 mmol) was added. The mixture was stirred for 15 h. Solvent was then removed under oil pump vacuum. The resulting dark yellow powder was dissolved in CH₂Cl₂ (4 mL), and the mixture was filtered through a glass plug. Ether (15 mL) was added to the filtrate with stirring. A bright yellow powder formed, which was washed with ether (3 × 2 mL)[43] to give 2a⁺BF₄⁻ (0.040 g, 0.057 mmol, 83%).

Variable-Temperature NMR Spectroscopy. Dynamic NMR studies were conducted in sealed tubes on Varian XL-300 spectrometers, as previously described.[31a] Samples were thoroughly degassed (freeze–pump–thaw × 3), and probe temperatures were calibrated with methanol.

Crystal Structures. The solvate 2a⁺TfO⁻·CH₂Cl₂ was crystallized a second time as described above. A yellow prism was mounted on a glass fiber for preliminary data collection on a Syntex PĪ diffractometer. Cell constants (Table II) were determined from 15 centered reflections with $12° \leq 2\theta \leq 30°$. Lorentz, polarization, and empirical absorption corrections were applied to the data. The structure was solved by standard heavy-atom techniques using the SDP/VAX package.[45] Hydrogen atom positions were calculated. Non-hydrogen atoms were refined with anisotropic thermal parameters. Anomalous dispersion corrections were applied through the refinement. Scattering factors and $\Delta f'$ and $\Delta f''$ values were taken from the literature.[46] The crystal structures of 4a⁺BF₄⁻ and 6a⁺TfO⁻ were solved in a similar manner, except that several triflate atoms in 6a⁺TfO⁻ were refined isotropically.

Supplementary Material Available: Tables of anisotropic thermal parameters for 2a⁺TfO⁻·CH₂Cl₂, 4a⁺BF₄⁻, and 6a⁺TfO⁻ (3 pages); tables of calculated and observed structure factors for 2a⁺TfO⁻·CH₂Cl₂, 4a⁺BF₄⁻, and 6a⁺TfO⁻ (72 pages). Ordering information is given on any current masthead page.

(45) Frenz, B. A. The Enraf-Nonius CAD 4 SDP—A Real-time System for Concurrent X-ray Data Collection and Crystal Structure Determination. In *Computing and Crystallography*; Schenk, H., Olthof-Hazelkamp, R., von Konigsveld, H., Bassi, G. C., Eds.; Delft University Press: Delft, Holland, 1978; pp 64–71.

(46) Cromer, D. T.; Waber, J. T. In *International Tables for X-ray Crystallography*; Ibers, J. A., Hamilton, W. C., Eds.; Kynoch: Birmingham, England, 1974; Volume IV, pp 72–98, 149–150, Tables 2.2B and 2.3.1.

Acidolysis of [MeC(CH₂PPh₂)₃]Rh(CH₃)ₙ Compounds: Controlled Creation of Unsaturation

David J. Rauscher, Eric G. Thaler, John C. Huffman, and Kenneth G. Caulton*

Department of Chemistry and Molecular Structure Center, Indiana University, Bloomington, Indiana 47405

Reaction of (triphos)RhMe₃ (triphos = MeC(CH₂PPh₂)₃) with HBF₄·OEt₂ in CH₂Cl₂ gives (triphos)-RhMe₂BF₄, which readily adds MeCN and reacts with CO to give acetone and (triphos)Rh(CO)₂⁺. When the protonation product is treated with 100 psi of C₂H₄, (triphos)Rh(C₂H₄)₂⁺ is produced. This cation is intramolecularly fluxional and exchanges readily with ¹³C₂H₄. The ethylene is weakly bound and is readily replaced by water to give [(triphos)Rh(C₂H₄)(H₂O)]BF₄, whose structure was established by X-ray diffraction. Crystallographic data (–172 °C): $a = 10.502$ (2) Å, $b = 16.518$ (4) Å, $c = 24.210$ (5) Å, and $\beta = 97.81$ (1)° with $Z = 4$ in space group $P2_1/c$. The trigonal-bipyramidal rhodium has C₂H₄ equatorial and H₂O axial. The water hydrogen bonds to BF₄ (O···F = 2.665 Å). Added ethylene will, in turn, displace coordinated water. This same compound is formed on protonation of (triphos)RhMe(C₂H₄) in the presence of ethylene and water. Protonation of (triphos)RhMe(C₂H₄) in the presence of acetonitrile yields (triphos)Rh-(NCCH₃)(C₂H₄)⁺, which has acetonitrile in an axial position. Analysis of variable-temperature ¹H, ¹³C, and ³¹P NMR data for these 18-electron cations suggests that they react by preliminary "arm-off" dissociation of one of the three phosphorus donor groups.

Introduction

Acidolysis of an organo-transition metal compound[1–4] (eq 1) can be an effective method for creating an open coordination site, since it formally removes R⁻. This

$$MR_xL_n + H^+ \xrightarrow{-RH} MR_{x-1}L_n^+ \tag{1}$$

process generates a transient 16e⁻ species that may be stabilized by the solvent or an available counterion (conjugate base of the acid employed). These formally unsaturated species are much more reactive toward a variety of nucleophiles (e.g., CO, MeCN, olefin, alkyne, etc.) than are their saturated precursors in eq 1. In the case of IrR₃(PMe₂Ph)₃ (R = H[3] or Me[3,4]) complexes, activation

(1) Rhodes, L. F.; Zubkowski, J. D.; Folting, K.; Huffman, J. C.; Caulton, K. G. *Inorg. Chem.* **1982**, *21*, 4185.

(2) Crabtree, R. H.; Haltky, G. G.; Parnell, C. P.; Segmüller, B. E.; Uriarte, R. J. *Inorg. Chem.* **1984**, *23*, 354.

(3) Lundquist, E. G.; Huffman, J. C.; Folting, K.; Caulton, K. G. *Angew. Chem., Int. Ed. Engl.* **1988**, *27*, 1165.

(4) Lundquist, E. G.; Folting, K.; Huffman, J. C.; Caulton, K. G. *Organometallics* **1990**, *9*, 2254.